ELSEVIER

Biomaterials 22 (2001) 2705–2712

Biomaterials

www.elsevier.com/locate/biomaterials

Mechanochemical synthesis of nanocrystalline hydroxyapatite from CaO and $CaHPO_4$

K.C.B. Yeong[a,*], J. Wang[a], S.C. Ng[b]

[a]*Department of Materials Science, Faculty of Science, National University of Singapore, Singapore 119260, Singapore*
[b]*Department of Physics, Faculty of Science, National University of Singapore, Singapore 119260, Singapore*

Received 5 May 2000; accepted 14 July 2000

Abstract

Ceramic hydroxyapatite phase was triggered to occur by high-energy mechanical activation of a dry powder mixture of calcium oxide (CaO) and anhydrous calcium hydrogen phosphate ($CaHPO_4$). A singe-phase hydroxyapatite of high crystallinity was realised by >20 h of mechanical activation without further thermal treatment at high temperatures. The resulting hydroxyapatite powder exhibits an average particle size of ~ 25 nm and a specific surface area of 76.06 m^2/g, as measured by multi-point BET technique. It was sintered to a density of 98.20% theoretical density at 1200°C for 2 h. © 2001 Published by Elsevier Science Ltd.

Keywords: Mechanochemical synthesis; Nanocrystalline hydroxyapatite; CaO; $CaHPO_4$

1. Introduction

Hydroxyapatite (HA), is the main mineral constituent of vertebrate skeletal systems [1]. As a bioceramic material, ceramic hydroxyapatites are widely employed in various biomedical applications, which involve the exploitation of their excellent biocompatibility and surface active properties with living tissue [2–5]. For many of these biomedical applications, a dense ceramic material of hydroxyapatite composition, which exhibits the required mechanical properties for load bearing, is required. The fabrication of such a densely sintered ceramic almost always starts with the synthesis of a hydroxyapatite powder of desirable particle characteristics, characterised by fine and uniform particle size, preferably in the nanometer range, homogeneity in phase and chemical composition together with a minimised degree of particle agglomeration [6,7]. Therefore, a number of ceramic and chemistry-based novel processing routes have been developed for preparing fine and sintering-reactive hydroxyapatite powders, including precipitation and hydrolysis [8,9], refined solid state reactions [10], sol–gel syntheses [11,12], hydrothermal reactions [13,14], and emulsion and microemulsion syntheses [15,16].

Mechanochemical syntheses were originally designed for oxide dispersion-strengthened (ODS) alloys [17]. Over the past 20 years, they have grown and diverged and they are now used for the fabrication of a wide range of advanced materials, both metallic and non-metallic in composition. However, little work has been done in the case of crystalline hydroxyapatite phase, although mechanochemical reactions have been successful in the synthesis of several ceramic materials with novel properties [18–21]. The attempts for crystalline hydroxyapatite via mechanochemical reactions resulted in a calcium deficient composition of low crystallinity, which was transformed into either β-tricalcium phosphate [22] or a mixture of hydroxyapatite and β-tricalcium phosphate upon calcination at ~ 720°C [23]. The present work is aimed at investigating the feasibility of synthesizing crystalline hydroxyapatite via a new mechanical activation route with the following two objectives: (a) to form crystalline hydroxyapatite by mechanically activating a dry powder mixture of calcium oxide (CaO) and anhydrous calcium hydrogen phosphate ($CaHPO_4$); and (b) to study the phase stability, powder characteristics and sintering behaviour of the hydroxyapatite derived from mechanical activation.

* Correspondence address: Department of Physics, Faculty of Science, National University of Singapore, Singapore 119260, Singapore.

0142-9612/01/$ - see front matter © 2001 Published by Elsevier Science Ltd.
PII: S0142-9612(00)00257-X

2. Experimental procedures

The starting materials for this work were commercially available anhydrous calcium hydrogen phosphate ($CaHPO_4$, Merck $\geqslant$98%) and calcium oxide (Cao, GCE $\geqslant$96%). Appropriate amounts of the two starting materials at a molar ratio of 3 : 2 were mixed together in a conventional ball mill in ethanol with zirconia balls as the milling medium. The powder mixture was then loaded into an alumina vial of 37 mm in diameter and 40 mm in length, together with a stainless-steel ball of 12.7 mm in diameter. Mechanical activation was carried out in a high-energy shaker mill for various time periods, the detailed experimental set-ups of which have been described in Refs. [24,25].

Phases present in the powder compositions mechanically activated for various time periods were analyzed using an X-ray diffractometer (CuK_α, X'pert Diffractometer, Philips). Their particle sizes were calculated on the basis of specific surface areas, as measured using a BET surface area analyzer (NOVA 2000, Quantachrome). Thermal analyses (TGA, DTA) of the mechanically activated powders were carried out at a heating rate of 10°C/min in air from room temperature to 900°C (Dupont 2100 thermal analyzer). Their particle characteristics were studied using a transmission electron microscope (JOEL, 100CX).

To fabricate sintered hydroxyapatites, the powder derived from 25 h of mechanical activation was de-agglomerated in a conventional ball mill for 24 h in ethanol in order to remove hard agglomerates. The powder was then uniaxially pressed into pellets in a hardened steel die of 10 mm in diameter at a pressure of 25 MPa, followed by isostatic pressing at a pressure of 345 MPa, prior to sintering at various temperatures in the range of 900–1300°C. For this, both heating and cooling rates were fixed at 5°C/min. Sintered hydroxyapatite pellets were then characterized for density using the Archimedes method in distilled water, into which a few drops of wetting agent was added. They were then polished to 6 μm finish using diamond paste and tested for Vickers hardness using indentation technique (Shimadzu HSV-20). Scanning electron microscope (SEM, Philips XL30) was employed to study the microstructural features of sintered hydroxyapatites.

3. Results and discussion

Fig. 1 shows the XRD traces of the powder mixtures that were subjected to mechanical activation for various time periods ranging from 5 to 25 h, together with that of the starting powder mixture that was not subjected to any mechanical activation. For the latter, only sharp peaks characteristic of CaO, $Ca(OH)_2$ and $CaHPO_4$ are observed, indicating that little or no reaction took place between the starting constituent powders during the mixing by conventional ball milling. The occurrence of $Ca(OH)_2$ in the starting powder mixture is attributed to the transformation of CaO to $Ca(OH)_2$ due to the presence of moisture during the conventional ball milling and subsequent mechanical activation. For the powder that was subjected to 5 h of mechanical activation, all the sharp peaks corresponding to CaO and $Ca(OH)_2$ have vanished, and those corresponding to $CaHPO_4$ have been broadened, indicating that a significant refinement in crystallite and particle sizes of the starting powders had occurred, together with a degree of amorphization at the initial stage of mechanical activation. As the mechanical activation time is increased to 10 h, further refinement in crystallite and particle sizes and an increased degree of amorphization are observed as the diffraction peaks belonging to $CaHPO_4$ have further been broadened. Upon 15 h of mechanical activation, several new broadened peaks appear to emerge. The most prominent one is situated at 2θ angle of $\sim$31.8°, corresponding to hydroxyapatite (2 1 1) peak. This suggests that nanocrystallites of hydroxyapatite phase have been formed as a result of the mechanical activation. The two minor peaks observed at 2θ angles of 26.3 and 30.2° correspond to the (0 0 2) and (1 2 0) peaks of $CaHPO_4$, respectively. When the mechanical activation time is extended to 20 h, all the peaks corresponding to $CaHPO_4$ have disappeared and only those belonging to hydroxyapatite are

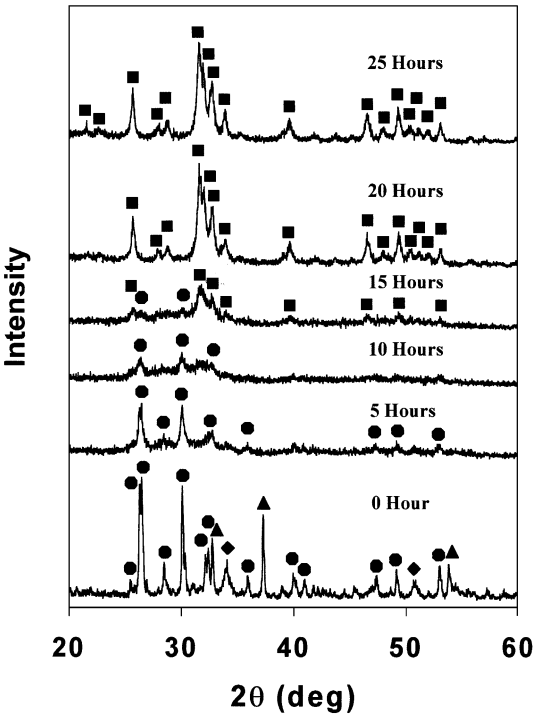

Fig. 1. XRD patterns of the powder mixtures consisting of CaO and $CaHPO_4$ that were subjected to 0–25 h of mechanical activation. [(▲): CaO, (●): $CaHPO_4$, (◆): $Ca(OH)_2$, (■): HA].

detectable. The crystallinity of the newly formed hydroxyapatite phase was further established by the apparent splitting of hydroxyapatite (2 1 1), (1 1 2) and (3 0 0) peaks over the 2θ angle range of 31.5–33.5°. Further increasing the activation time to 25 h results in a further increase in the crystallinity of hydroxyapatite, as evidenced by the further sharpening of the principal diffraction peaks.

In Table 1, the specific surface areas and corresponding particle sizes for the powders that were subjected to various hours of mechanical activation from 5 to 25 h, together with that for the powder that was not subjected to any mechanical activation are shown. A specific surface area of 8.65 m^2/g was measured for the powder that was activated for 5 h, in contrast to 4.76 m^2/g for the powder that was not subjected to any mechanical treatment. Apparently, nanosized hydroxyapatite particles had been formed in the powders that were mechanically activated for more than 20 h. This correlate well with the sharp and distinct diffraction peaks in XRD trace observed for the newly formed hydroxyapatite phase in these powders. An average particle size of ~25 nm was measured for the powder that was mechanically activated for 25 h.

Fig. 2(a) shows a bright field TEM micrograph of the powder mixture that was not subjected to any mechanical activation. It consists of $CaHPO_4$ agglomerates of 0.5–1.0 μm in size with irregular morphology together with the needle-like CaO particles of 0.5–2.0 μm in length. In contrast, in Fig. 2(b) for the powder mixture

Table 1
The specific surface area and equivalent particle size of the powders consisting of $CaHPO_4$, and CaO, upon mechanical activation for various time periods

Mechanical activation duration (h)	Specific surface area (m^2/g)	Equivalent particle size (nm)
0	4.76	—
5	8.65	—
10	9.47	—
15	9.89	191.99
20	66.86	28.40
25	76.06	24.96

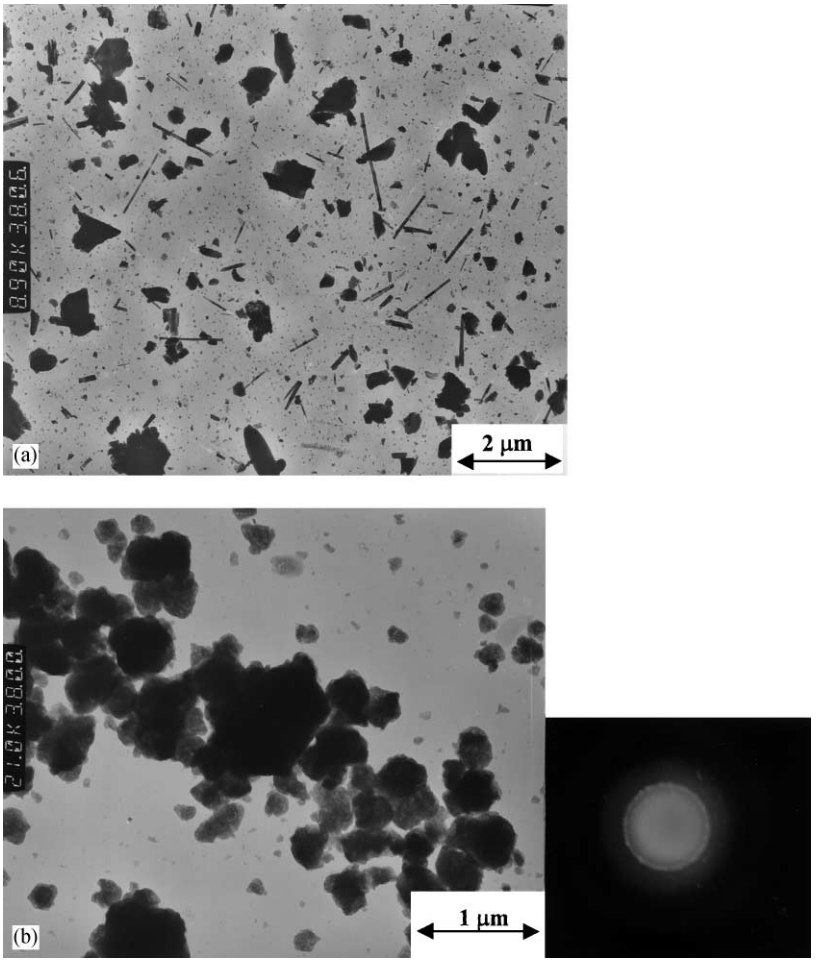

Fig. 2. (a) TEM of the powder that was not subjected to any mechanical activation. (b) TEM and SAD patterns of the powder that was subjected to 5 h of mechanical activation. (c) TEM and SAD patterns of the powder that was subjected to 15 h of mechanical activation. (d) TEM and SAD patterns of the powder that was subjected to 25 h of mechanical activation.

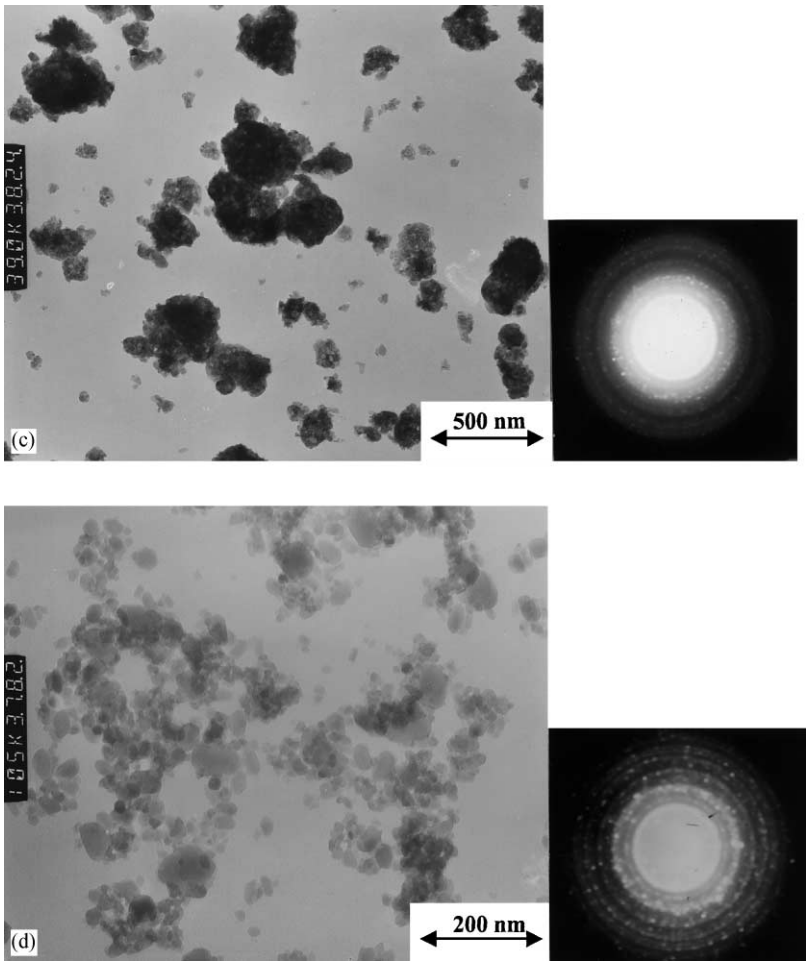

Fig. 2. (*Continued*).

that was subjected to 5 h of mechanical activation, particle agglomerates of 0.2–1.0 μm in sizes are observed. They exhibit a rather low degree of crystallinity as indicated by the diffused rings in SAD patterns. Fine discrete particles are clearly visible in these agglomerates. When mechanically activated for 15 h as shown in Fig. 2(c), these particle agglomerates are further refined in size and the corresponding SAD indicates that the powder consists of nanocrystallites. Upon further increase in mechanical activation time to 25 h, nanocrystallites of the newly formed hydroxyapatite phase are clearly observed by the selected area diffraction pattern. These particles, as seen in Fig. 2(d), exhibit a rounded morphology and they are 20–30 nm in size. This agrees with what has been shown by the phase analysis of XRD and BET specific surface area for the powder.

Fig. 3(a) illustrates the DTA and TGA curves for the powder mixture that was not subjected to any mechanical activation. Two apparent endothermic reactions accompanied by corresponding weight losses were observed at ~467 and 620°C, respectively. The first endothermic reaction is attributed to the transformation of $CaHPO_4$ to γ-$Ca_2P_2O_7$ [26], and the second one is due to the decomposition of a minor amount of $Ca(OH)_2$ present in the powder mixture to CaO prior to mechanical activation, respectively. In comparison, in Fig. 3(b) for the powder mixture that was subjected to 25 h of mechanical activation, no significant endothermic reactions were observed except for the one due to the loss of adsorbed moisture at the low temperature of ~100°C [27]. The TGA trace shows a steady and continuous weight loss from room temperature up to ~550°C. This is ascribed to the loss of absorbed moisture from the hydroxyapatite phase that had already been formed as a result of the mechanical activation [28]. The lack of any prominent endothermic reactions and weight losses over the temperature range studied for the powder mixture that was subjected to 25 h of mechanical activation suggests that the reaction between CaO and $CaHPO_4$ was largely completed by 25 h of mechanical activation at room temperature.

Mechanochemical reactions among solid powder constituents is a complicated process, and currently, no well-established theories exist for satisfactorily explaining many of the interesting phenomena observed [29]. However, from the experimental results of XRD phase

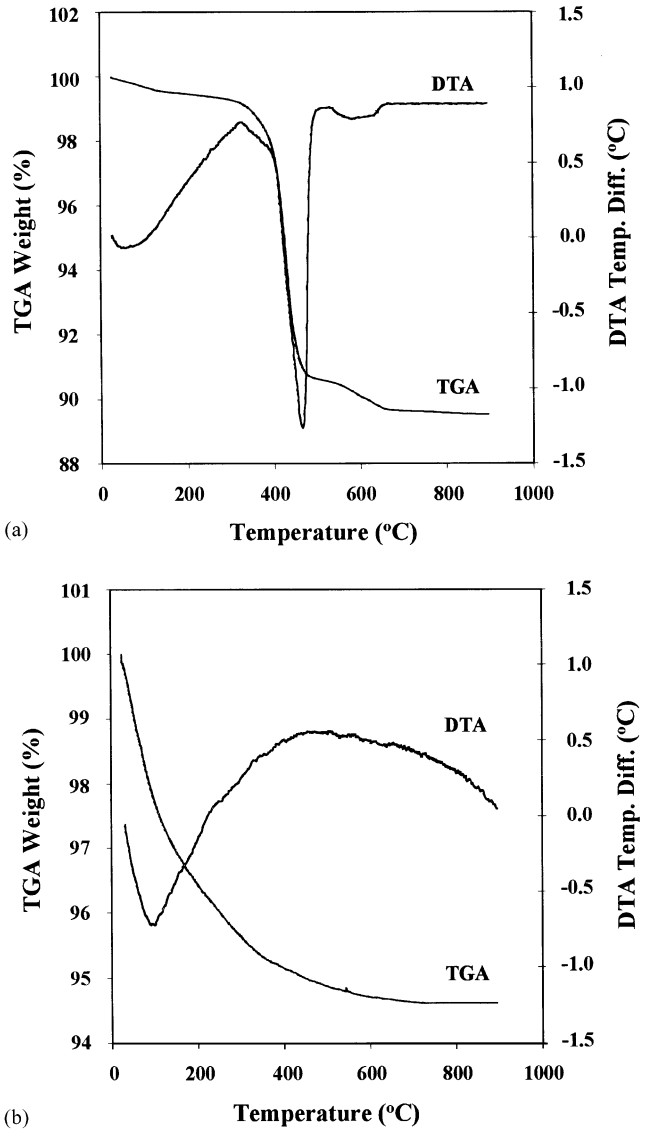

Fig. 3. (a) The DTA and TGA traces for the powder that was not subjected to any mechanical activation. (b) The DTA and TGA traces for the powder that was subjected to 25 h of mechanical activation.

analysis, BET specific surface measurement, TEM observation, TGA and DTA thermal analyses discussed above, two apparent processes occur when the powder mixture of calcium oxide and anhydrous calcium hydrogen phosphate is subjected to an increasing degree of mechanical activation:

(i) a dramatic increase in the specific surface area and refinement in the crystallite and particle sizes due to the fragmentation and fracture of starting particles, together with a degree of amorphization at the initial stage of mechanical activation; and
(ii) the solid-state reaction in the highly activated powder matrix at the subsequent stage of mechanical activation, leading to the formation and growth of hydroxyapatite crystallites.

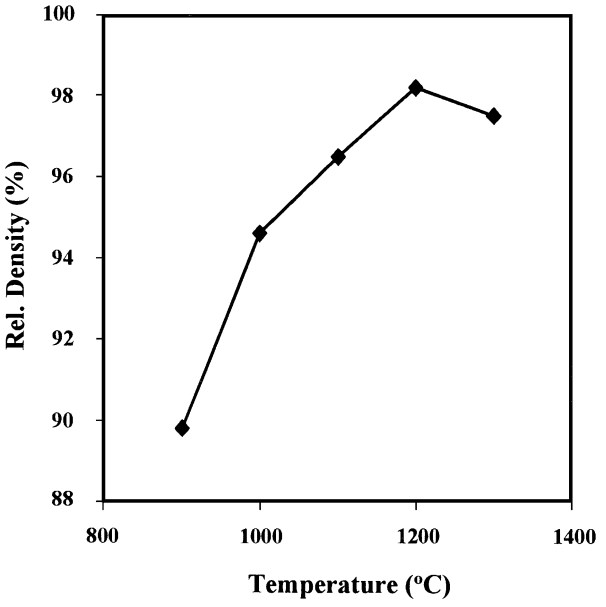

Fig. 4. Relative density of the HA derived from the powder subjected to 25 h of mechanical activation, as a function of sintering temperature in the range of 900–1300°C.

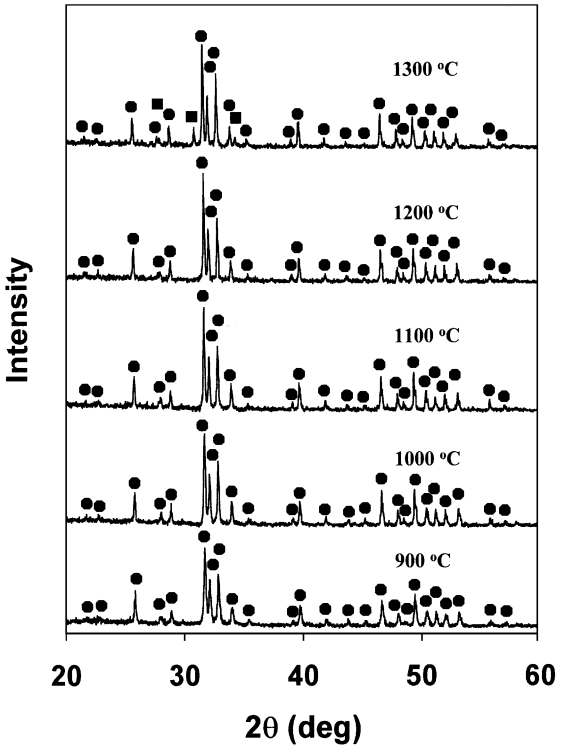

Fig. 5. XRD traces of the HA derived from the powder that was subjected to 25 h of mechanical activation and sintered at various temperatures ranging from 900 to 1300°C. [(●): HA, (■): β-tricalcium phosphate].

With increasing mechanical activation time at the initial stage, the refinement in crystallite and particle sizes of the constituent powders increases the population of point defects and lattice defects considerably. The

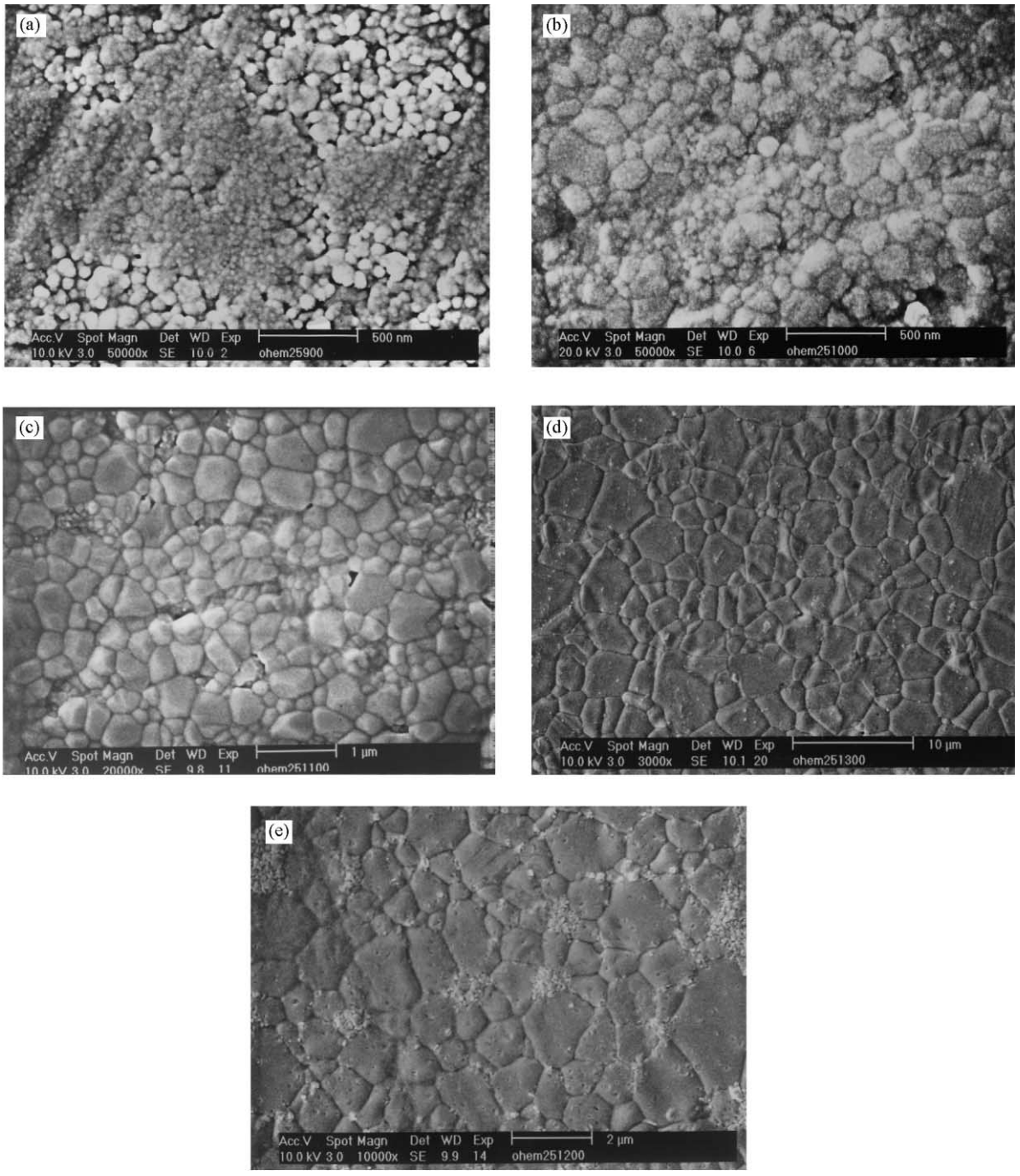

Fig. 6. (a) SEM micrograph of polished surface of the pellet derived from the powder that was mechanically activated for 25 h and then sintered at 900°C; (b) at 1000°C; (c) at 1100°C; (d) at 1200°C; (e) at 1300°C.

accumulation of these defects can result in a significant increase in their reactivities. Further mechanical activation leads to the formation and growth of hydroxyapatite nanocrystallites as a result of mechanochemical reaction, as evidenced by the increasing sharpness in XRD peaks as shown in Fig. 1. The high-impact compression [30,31] and the instantaneous increase in local temperature [32] at the collision points are the likely key contributing factors in triggering the solid-state reaction in a nanometer scale via enhanced diffusion processes. However, the measurements of local collision conditions in a high-energy mechanical activation process is extremely difficult and subjective to the methods of measurement. Therefore, complete verification of such a theory is still tentative and not fully explored.

Fig. 4 plots the sintered density as a function of sintering temperature for the hydroxyapatite derived from the powder that was subjected to 25 h of mechanical

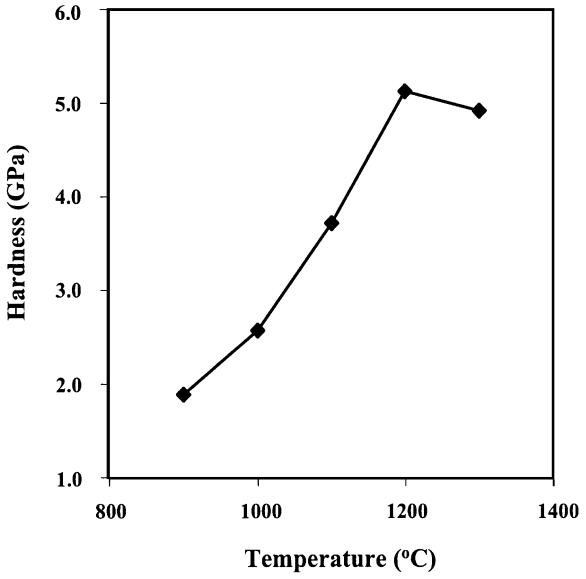

Fig. 7. The Vickers Hardness of the HA derived from the powder that was mechanically activated for 25 h as a function of sintering temperature.

activation. A steady rise in the sintered density is observed when the sintering temperature is raised from 900 to 1000°C. The sintered density continues to increase with increasing sintering temperature up to 1200°C, where it maximises at 98.20% theoretical density. Further increase in the sintering temperature to 1300°C results in a slight fall in the sintered density to 97.50% theoretical density. This is attributed to the partial decomposition of hydroxyapatite beyond 1200°C, which has been confirmed by the phase analysis using XRD, as shown in Fig. 5.

The microstructural features of sintered hydroxyapatites derived from the powder that was subjected to 25 h of mechanical activation and sintered at various temperatures ranging from 900 to 1300°C are shown in Figs. 6(a)–(e), respectively. When sintered at 900°C, a non-uniform distribution of grains with size in the range of 20–130 nm was observed. The sintered structure consists of differential areas of coarse grains of ~100 nm, together with very fine grains of ~20 nm. When the sintering temperature was increased to 1000°C, the grain size distribution was apparently narrowed together with an increase in grain size to 150–200 nm. Further increasing the sintering temperature to 1100°C results in an apparent rise in the average grain size, to 0.2–0.5 μm, together with a rather dense microstructure developed. Sintering at 1200°C led to the formation of a very dense microstructure with grains in the range of 2.0–5.0 μm in size. This accounts for the high sintered density of ~98% theoretical for the hydroxyapatite sintered at 1200°C. However, upon further increasing the sintering temperature to 1300°C, the occurrence of secondary phases consisting of fine particles of ~100 nm was observed among the coarse hydroxyapatite grains. This is ascribed to the decomposition of hydroxyapatite at 1300°C, forming fine β-tricalcium phosphate particles as indicated by the phase analysis detailed in Fig. 5.

Fig. 7 illustrates the dependence of Vickers hardness of sintered hydroxyapatite derived from 25 h of mechanical activation on sintering temperature. The hardness increases almost linearly with rising sintering temperature from 900 to 1200°C, where it reaches a maximum of 5.12 GPa. This is followed by a slight decrease, to 4.92 GPa, when the sintering temperature is raised to 1300°C. Apparently, the dependence of hardness more or less follows what has been observed for the sintered density as a function of sintering temperature, as the hardness is strongly affected by the sintered density.

4. Conclusions

Nanocrystalline hydroxyapatite phase has been triggered to form by high-energy mechanical activation in a dry powder mixture of calcium oxide (CaO) and anhydrous calcium hydrogen phosphate ($CaHPO_4$). The initial stage of mechanical activation resulted in a significant refinement in crystallite and particle sizes, together with a degree of amorphization in the starting powder mixture. This is followed by steady formation and subsequent growth of hydroxyapatite crystallites with increasing degree of mechanical activation. A singe-phase hydroxyapatite of high crystallinity was attained by >20 h of mechanical activation. The resulting hydroxyapatite powder exhibits an average particle size of ~25 nm. It was sintered to a density of 98.20% theoretical density at 1200°C for 2 h.

References

[1] de Groot K. Bioceramics consisting of calcium phosphate salts. Biomaterials 1980;1:47–50.
[2] Hench LL. Bioceramics: from concept to clinic. J Am Ceram Soc 1991;74:1487–510.
[3] Aoki H. Medical applications to hydroxyapatite. Ishiyaku Euro-America: Tokyo, 1994; p. 133–54.
[4] Lin FH, Lin CC, Liu HC, Huang YY, Wang CY, Lu CM. Sintered porous DP-bioactive glass and hydroxyapatite as bone substitute. Biomaterials 1994;15:1087–98.
[5] Klein CPAT, de Blieck-Hogervorst JMA, Wolke JGC, de Groot K. Studies of the solubility of different calcium phosphate ceramic particles invitro. Biomaterials 1990;11:509–12.
[6] Best S, Bonfield W, Doyle DC. A study into the preparation of dense hydroxyapatite ceramics using powders of different morphologies. In: Oonishi H, Aoki H, Sawai K, editors. Bioceramics, Proceedings of the First International Bioceramics Symposium. Ishiyaku Euro-America: Tokyo, 1989. p. 68–73.
[7] Lange FF. Powder processing science and technology for increased reliability. J Am Ceram Soc 1989;72:3–15.
[8] Puajindanetra S, Best SM, Bonfield W. Characterisation and sintering of precipitated hydroxyapatite. Br Ceram Trans J 1994;93:96–9.

[9] Lopez-Macipe A, Rodriguez-Clemente R, Hidalgo-Lopez A, et al. Wet chemical synthesis of hydroxyapatite particles from nonstoichiometric solutions. J Mater Synth Process 1998;6: 21–6.
[10] Fowler BO. Infrared studies of apatites II. Preparation of normal and isotopically substituted calcium, strontium and barium hydroxyapatite and spectra-structure-composition correlations. Inorg Chem 1974;13:207–14.
[11] Deptula A, Lada W, Olczak T, Borello A, Alvani C, Dibartolomeo A. Preparation of spherical powders of hydroxyapatite by sol-gel process. J Non-Cryst Solids 1992;147:537–41.
[12] Vallet-Regi M, Gutierrez-Rios MT, Alonso MP, de Frutos MI, Nicolopoulos S. Hydroxyapatite particles synthesised by pyrolosis of an aerosol. J Solid State Chem 1994;112:58–64.
[13] Hattori H, Iwadate Y. Hydrothermal preparation of calcium hydroxyapatite powders. J Am Ceram Soc 1990;73:1803–5.
[14] Yoshimura M, Suda H, Okamoto K, Ioku K. Hydrothermal synthesis of biocompatible whiskers. J Mater Sci 1994;29: 3399–402.
[15] Murray MGS, Wang J, Ponton CB, Marquis PM. An improvement in processing of hydroxyapatite ceramics. J Mater Sci 1995; 30:3061–74.
[16] Lim GK, Wang J, Ng SC, Gan LM. Processing of fine hydroxyapatite powders via an inverse microemulsion route. Mater Lett 1996;30:431–6.
[17] Benjamin JS. Mechanical alloying. Sci Am 1976;234:40–8.
[18] Abe O, Suzuki Y. Mechanochemically assisted preparation of $BaTiO_3$ powder. Mater Sci Forum 1996;225:563–8.
[19] Puclin T, Kaaczmarek WA, Ninham BW. Mechanochemical processing of $ZrSiO_4$. Mater Chem Phys 1995;40:70–81.
[20] Ding J, Miao WF, McCormick PG, Street R. Mechanochemical synthesis of ultrafine Fe powders. Appl Phys Lett 1995; 67:3804–6.
[21] Hamada K, Senna J. Mechanochemical effects on the properties of starting mixtures of $PbTiO_3$ ceramics by using a novel grinding equipment. J Mater Sci 1996;31:1725–8.
[22] Toriyama M, Kawamura S. Sinterable powder of mechanochemically synthetic β-tricalcium phosphate. Yogyo-Kyokai-Shi 1987; 95:698–702.
[23] Toriyama M, Ravaglioli A, Krajewski A, Celloti G, Piancastelli A. J Eur Ceram Soc 1996;16:429–36.
[24] Lee SE, Xue JM, Wan DM, Wang J. Effects of mechanical activation on the sintering and dielectric properties of oxide-derived PZT. Acta Mater 1999;47:2633–9.
[25] Xue JM, Tan YL, Wan DM, Wang J. Synthesising 0.9PZN-0.1BT by mechanically activating mixed oxides. Solid State Ion 1999; 120:183–9.
[26] Yang X, Wang Z. Synthesis of biphasic ceramics of hydroxyapatite and β-tricalcium phosphate with controlled phase content and porosity. J Mater Chem 1998;8:2233–7.
[27] LeGeros RZ, Bonel G, Legros R. Types of "H_2O" in human enamel and in precipitated apatites. Calcif Tissues Res 1978; 26:111–8.
[28] Young RA, Holcomb DA. Role of acid phosphate in hydroxyapatite lattice expansion. Calcif Tissue Int 1984;36:60–3.
[29] Koch CC. Materials synthesis by mechanical alloying. Annu Rep Mater Sci 1989;19:121–42.
[30] Shen TP, Koch CC, McCormick TL, Nemanich RJ, Huang JY, Huang JG. The structure and property characteristics of amorphous/nanocrystalline silicon produced by ball milling. J Mater Res 1995;10:139–48.
[31] Thadhani NN. Shock-induced and shock-assisted solid-state chemical reactions in powder mixtures. J Appl Phys 1994; 76:2129–38.
[32] Schwarz RB. Introduction to the viewpoint set on: mechanical alloying. Scrip Mater 1996;34:1–4.